ISSN 1063-7826, Semiconductors, 2008, Vol. 42, No. 1, pp. 99–103. © Pleiades Publishing, Ltd., 2008.
Original Russian Text © L.D. Moldavskaya, N.V. Vostokov, D.M. Gaponova, V.M. Danil'tsev, M.N. Drozdov, Yu.N. Drozdov, V.I. Shashkin, 2008, published in Fizika i Tekhnika Poluprovodnikov, 2008, Vol. 42, No. 1, pp. 101–105.

PHYSICS OF SEMICONDUCTOR DEVICES

# The Sandwich InGaAs/GaAs Quantum Dot Structure for IR Photoelectric Detectors

**L. D. Moldavskaya^, N. V. Vostokov, D. M. Gaponova, V. M. Danil'tsev, M. N. Drozdov, Yu. N. Drozdov, and V. I. Shashkin**

*Institute of Physics of Microstructures, Russian Academy of Sciences, Nizhni Novgorod, 603950 Russia*
*^e-mail: lmd@ipm.sci-nnov.ru*

Submitted April 11, 2007; accepted for publication April 19, 2007

**Abstract**—A new possibility for growing InAs/GaAs quantum dot heterostructures for infrared photoelectric detectors by metal–organic vapor-phase epitaxy is discussed. The specific features of the technological process are the prolonged time of growth of quantum dots and the alternation of the low- and high-temperature modes of overgrowing the quantum dots with GaAs barrier layers. During overgrowth, large-sized quantum dots are partially dissolved, and the secondary InGaAs quantum well is formed of the material of the dissolved large islands. In this case, a sandwich structure is formed. In this structure, quantum dots are arranged between two thin layers with an increased content of indium, namely, between the wetting InAs layer and the secondary InGaAs layer. The height of the quantum dots depends on the thickness of the GaAs layer grown at a comparatively low temperature. The structures exhibit intraband photoconductivity at a wavelength around 4.5 μm at temperatures up to 200 K. At 90 K, the photosensitivity is 0.5 A/W, and the detectivity is $3 \times 10^9$ cm $Hz^{1/2}$ $W^{-1}$.

PACS numbers: 68.65.Hb, 73.50.Pz, 73.63.Kv, 78.55.Cr, 78.67.Hc, 81.15.Gh

**DOI:** 10.1134/S1063782608010144

## 1. INTRODUCTION

In recent years, new approaches to the engineering of heterostructures with quantum dots (QDs) for infrared (IR) photoelectric detectors (PDs) on the basis of the InGaAs system have been suggested. Among the approaches are the development of the heterostructures such as QDs in quantum wells (QWs), superlattices of QD layers, and structures with extra barriers and tunneling-coupled QWs [1–7]. The studies in this field are carried out with the aim of extending the operating temperature range of IR PDs, to enhance their sensitivity, to reduce dark currents, and to extend the possibilities of controlling the spectral regions. The above-mentioned approaches involve the already developed processes of fabrication of QDs and the processes of modification of the regions surrounding the QDs. In this study, we discuss a new approach to the formation of QD structures for IR PDs. The approach is based on the direct modification of the arrays of QDs. For this purpose, we use the procedure of overgrowing of QDs with alternation of the temperature of growth of the GaAs barrier layers; in addition, we use the increased equivalent thickness of the InAs layer ($d^*$) to form the QDs. Previously [8], we observed a pronounced enhancement (30 times higher intensity) of the line of longitudinal intraband photoconductivity around the wavelength 4.5 μm as the equivalent thickness of the InAs layer was doubled. As the thickness $d^*$ was increased further, we observed two-color photoconductivity at the wavelengths 4.5 and 3 μm. We consider these results to be a consequence of the increase in the density of QDs and the formation of an array of larger nanoislands at larger values of $d^*$. At the same time, as far as we know, there are no studies concerned with the application of such structures to the development of IR PDs. As shown in [9–13], along with the increase in the density of QDs with increasing $d^*$, the dispersion of the QDs in size and the number of large-sized relaxed defect InAs clusters increase as well. This causes the photoluminescence (PL) line of the QDs to broaden and to reduce its intensity. For this reasons, such an approach is considered to have no prospects for producing laser structures. However, as noted in [8, 14], the performance criteria for laser structures, especially the intense PL signal, are inapplicable to IR PDs, since high intraband photoconductivity can be observed along with the low-intensity interband PL signal. In this study, we have fabricated a series of structures differing in the conditions of formation of QDs and in the conditions of overgrowth of the QDs with GaAs grown at relatively low temperatures. We study the structural and optical properties of these samples and perform the absolute calibration of their photosensitivity in the vertical layout of electronic transport.

## 2. QD STRUCTURES: FABRICATION AND CHARACTERIZATION

The multilayered InGaAs/GaAs QD heterostructures were grown by metal–organic vapor-phase epitaxy (MOVPE) at reduced pressure using an EPIQUIP

Parameters of growth of the QD structures

| Sample no. | Time of growth of QDs ($t^*$), s | Time of growth of low-temperature GaAs layer, s |
|---|---|---|
| 1060 | 12 | 20 |
| 1064 | 15 | 20 |
| 1061 | 18 | 20 |
| 1062 | 12 | 10 |
| 1063 | 12 | 30 |

VP-502RP system. For substrates, we used the GaAs (100) wafers, with the crystal cut tilted 2° towards the $[1\bar{1}0]$ direction. The structures consist of ten layers of selectively doped InAs QDs separated by GaAs barrier layers with thickness 60–90 nm. The doping δ-Si layers were formed at the distance of 2.5 nm under each layer of QDs. The InAs QDs were grown at the reduced temperature 480°C. Thereafter, the reactor was purged, and the QDs were overgrown by a thin GaAs layer at the same temperature of growth. After purging the reactor a second time, the temperature was elevated to 600°C, and the GaAs barrier layers were grown. The crucial parameters here are the time $t^*$ of growth of the QD or the equivalent thickness $d^*$ of the InAs layer. Of great importance is also the choice of the time point, at which the temperature has to be elevated. The "low-temperature" GaAs layer serves to conserve the QDs at further elevated temperature. At the same time, this procedure of growth involves the stage of dilution of large-sized defect clusters, as suggested recently in fabricating laser structures [15–18]. To analyze the samples by atomic force microscopy (AFM), the QDs were formed also at the surface of each structure and then overgrown by the "low-temperature" GaAs layer under the same conditions as those used in overgrowing the QDs within the structure. The parameters of growth are listed in the table.

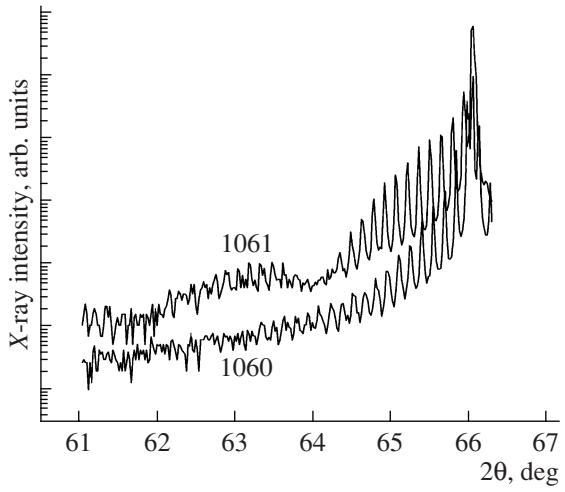


**Fig. 1.** XRD curves for structures 1060 and 1061.

To study the structures, we used a number of methods, including AFM, X-ray diffraction (XRD) studies, and PL measurements. The IR photoconductivity was studied using an INFRALUM FT-801 Fourier spectrometer. For the source of IR radiation, we used a globar at the temperature 1000°C. The absolute calibration of the photosensitivity was carried out with the use of an ideal blackbody source at the temperature 600°C.

## 3. XRD ANALYSIS

Figure 1 shows the XRD rocking curves for structures numbered 1060 and 1061. For structures 1060 and 1061, at the constant flux of In atoms in the reactor, the time of growth of InAs QDs $t^*$ was 12 and 18 s, respectively. For both structures, the time of growth of the "low-temperature" GaAs layer was 20 s. In structure 1061, the additional thickness-related contrast is observed, suggesting that the secondary $In_xGa_{1-x}As$ layer appears on top of the "low-temperature" GaAs layer and QDs. The numerical simulation of the XRD data allows us to estimate the thickness $d_2$ of this secondary layer and the compositional parameter $x_2$ characterizing the In content in this layer: $d_2 = 3.5$ nm and $x_2 = 9\%$. According to the XRD data, the thickness of the "low-temperature" GaAs layer is 6 nm. Thus, in structure 1061, the QDs are arranged between the two thin layers with a higher In content, the wetting InAs layer and the secondary $In_xGa_{1-x}As$ layer, thus forming a sandwich-like structure. It is worth noting that the observation of the secondary $In_xGa_{1-x}As$ layer by transmission electron microscopy (TEM) and by high-vacuum scanning tunneling microscopy (STM) of cleaved surfaces was reported previously in [18] (TEM) and [19] (STM). The above mechanism of MOVPE growth is as yet poorly known [20], although it may be of considerable interest for fabricating high-density arrays of QDs.

## 4. AFM STUDIES

Figure 2a shows the AFM image of the surface of sample 1060. In the image, we can see the overgrown QDs of high density, with insignificant contrast, and a few large-sized clusters. Among the QDs, there exist a small number of objects extended along the $[1\bar{1}0]$ direction, with depressions in the middle. The density of the objects of this type is much higher in structure 1062, in which the thickness of the "low-temperature" GaAs layer is twice as small (Fig. 2b). From Fig. 2b, it can be also seen that the QDs are ordered along the atomic steps of the vicinal surface. In publications, the images of this kind are referred to as "eye-like" patterns. The formation of such patterns suggests that the process of overgrowing the QDs occurs due to surface migration of atoms along the atomic steps at the surface of the

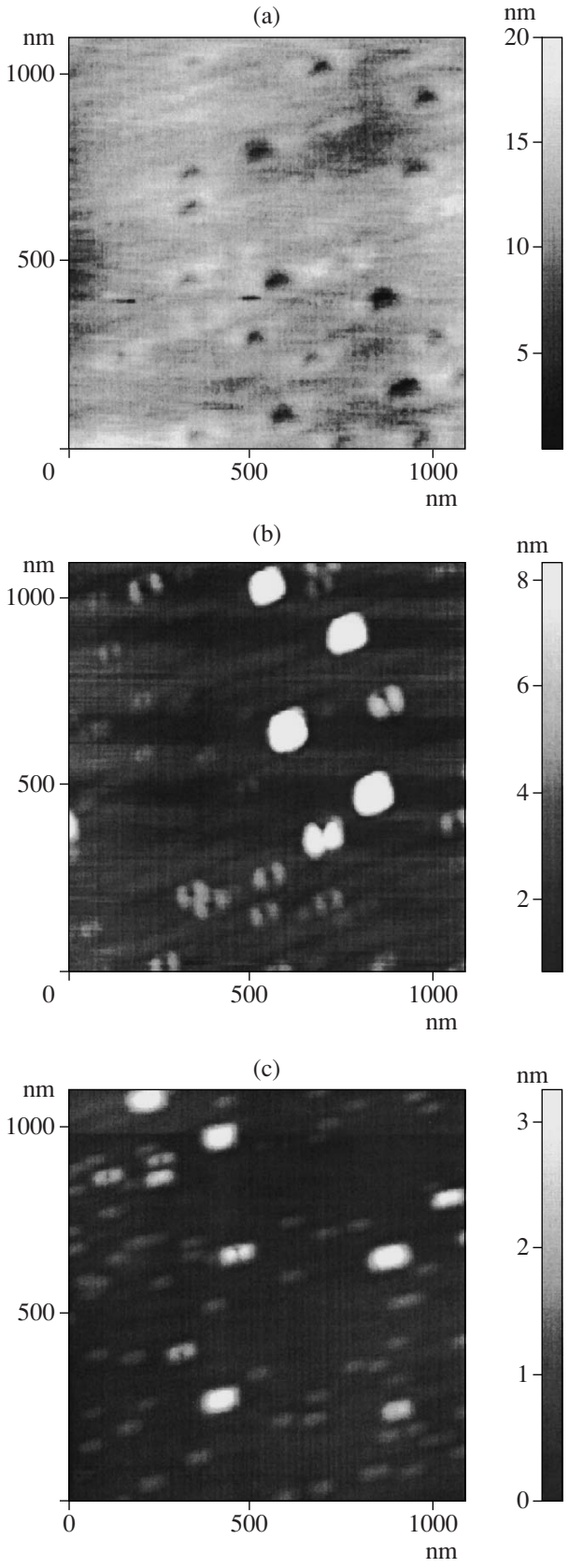


**Fig. 2.** AFM images of the surface of structures (a) 1060, (b) 1062, and (c) 1060 after annealing.

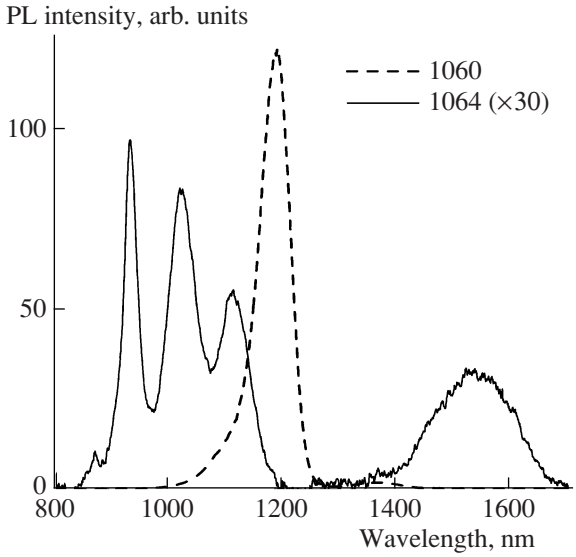


**Fig. 3.** PL spectra of structures 1060 and 1064 at 300 K. The excitation wavelength and power are 514.5 nm and 100 mW, respectively.

GaAs layer [21–23]. Therefore, at the early stages of overgrowth, this process is anisotropic. In contrast to the modes of overgrowth discussed in [22], under the conditions used here, no dilution of QDs occurs at the stage of overgrowth of the QDs by the "low-temperature" GaAs layer. Figure 2c shows the AFM image of the surface of sample 1060 after additional annealing at 600°C. It is evident that cavities are produced at the sites of large-sized clusters; i.e., the large-sized InAs clusters not overgrown before annealing dilute on annealing. This process is referred to as annealing of defects. Recently, the process was coming into use for manufacturing laser structures by molecular beam epitaxy (MBE) and MOVPE (see, e.g., [15–18]). In structure 1064, the number of large-sized clusters at the surface is larger than that in structure 1060; however, even in structure 1064, these clusters disappear on annealing as well. Thus, annealing of defects makes it possible also to reduce the number of defects in the structures with the increased thickness $d^*$ of the InAs layer. The In atoms of diluted clusters diffuse over the surface of the GaAs layer. As the barrier layer grows further, these In atoms form the secondary InGaAs layer.

## 5. PHOTOLUMINESCENCE OF QDs

Figure 3 shows the PL spectra of structures 1060 and 1064 at 300 K. For structure 1060, the wavelength corresponding to the basic transition in the QD, $\lambda_0$, is 1.2 μm. For structure 1064 ($t^*$ = 15 s), the spectrum exhibits an addition PL line at 1.55 μm, suggesting that these are QDs larger in size; at the same time, the PL intensity corresponding to small-sized QDs is much lower. It should be noted that the 1.55 μm line is retained when the upper 0.2- μm-thick layer of GaAs is

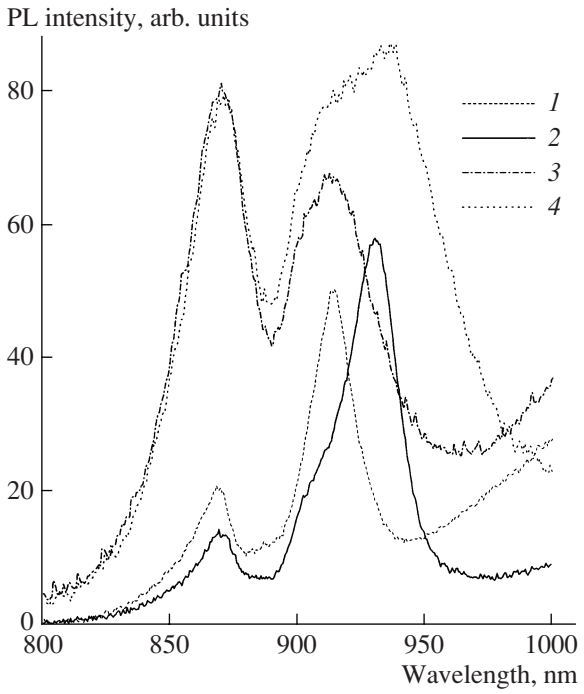


**Fig. 4.** PL spectra of structures (*1*, *3*) 1060 and (*2*, *4*) 1064. Curves *1* and *2* refer to excitation with an Ar laser (514.5 nm) and curves *3* and *4* to excitation with a YAG:$Nd^{3+}$ laser (532 nm).

chemically etched off (in this case, both the surface layer and the two layers of QDs below it inside the structure are etched off). This result indicates that the 1.55 μm line corresponds to large-sized QDs in the bulk of the structure rather than to QDs at the surface, as was observed, e.g., in [13, 24]. It is these QDs that are responsible for the photoconductivity at the wavelength around 3 μm, as we observed in [8].

As the duration of overgrowth of the QDs by a "low-temperature" GaAs layer is changed, the PL line of the QDs shifts. The wavelength of the basic transition in the QDs decreases to $\lambda_0 = 1.15$ μm as the GaAs layer is made thinner, and increases to $\lambda_0 = 1.27$ μm with increasing thickness of the GaAs layer; in both cases, the intensity and width of the PL line change only slightly. This proves that the height of the QDs depends directly on the thickness of the "low-temperature" GaAs layer. Thus, under the conditions of growth here, not only large-sized defect clusters, but also the tops of some large-sized coherent QDs can be diluted. The latter effect results in equalization of the array of QDs in height. Such a role of overgrowth was mentioned for the QDs at the surface in [25]. Due to this role, the overgrowth provides an additional means of controlling the PL wavelength and the operating wavelength of IR PDs. In addition, the overgrowth can yield an increase in the aspect ratio, i.e., in the ratio of the height to lateral dimension of the QDs. This effect is important for enhancing the photosensitivity and reducing the dark current of IR PDs [26].

Figure 4 shows the PL spectrum of the wetting layer in structures 1060 and 1064 under different conditions of excitation. On excitation with a cw Ar laser and a high-power pulsed YAG:$Nd^{3+}$ laser, the PL spectrum of structure 1060 exhibits one line of the QW at the wavelength about 914 nm (curves *1*, *3*). For structure 1064 excited with an Ar laser (curve *2*), we observe the 930 nm line of the QW and a low-intensity short-wavelength shoulder near 911 nm. The intensity of the short-wavelength line at 911 nm becomes noticeably higher when the sample is excited with the pulsed YAG:$Nd^{3+}$ laser (curve *4*). This is due to the more efficient occupation of the upper levels. We believe that this result gives supplementary evidence for the formation of the secondary InGaAs layer in the structure with larger $d^*$. The PL lines observed for structure 1064 are related to the levels in the two types of QWs, in the wetting InAs layer and in the additional InGaAs layer. It should be noted that the intensities of the PL lines of the QWs in structures 1060 and 1064 are almost the same, suggesting that, in structure 1064, the possible defects influence the PL signal only slightly.

## 6. ABSOLUTE CALIBRATION OF IR PHOTOCONDUCTIVITY

In order to study the vertical photoconductivity, we fabricated several QD structures at conducting substrates; the structures differed in the thickness $d^*$ of the equivalent InAs layer. In this case, we observe the same tendency in the evolution of the vertical photoconductivity with increasing $d^*$ as that noticed previously in analyzing the longitudinal photoconductivity [8]. At larger $d^*$, the photoconductivity is higher, and at the same time, the signal-to-noise ratio is noticeably improved. For the structure similar to structure 1064, the power–voltage sensitivity is $2 \times 10^4$ V/W in the wavelength range 3–6 μm at the temperature 90 K (the power–current sensitivity is 0.5 A/W), and the specific detectivity is $3 \times 10^9$ cm $Hz^{1/2}$ $W^{-1}$. This result is highly competitive with the best data obtained for QD structures grown by MOVPE [27].

## 7. CONCLUSIONS

By analogy with the known term "QDs in a QW", the structures studied here can be referred to as "QDs in a sandwich". The procedure of growth discussed above makes it possible to format high-density arrays of QDs, with a uniformly distributed height and a large aspect ratio. The procedure makes it possible to control the basic electronic transition in the QDs by varying the thickness of the overgrowing layer. The "low-temperature" GaAs layer (apparently of the *p*-type) serves as an extra barrier to reduce the dark current in the case of vertical charge transport. The studies of the photosensi-

tivity and detectivity show that such structures offer promise as IR detectors.

## ACKNOWLEDGMENTS

The study was supported by the Russian Foundation for Basic Research, project nos. 06-02-16519 and 07-02-00163.

## REFERENCES

1. W. Zhang, H. Lim, M. Taguchi, et al., Appl. Phys. Lett. **86**, 191103 (2005).
2. D. Pal and E. Towe, Appl. Phys. Lett. **88**, 153109 (2006).
3. S. Chakrabarti, A. D. Stiff-Roberts, X. H. Su, et al., J. Phys. D: Appl. Phys. **38**, 2135 (2005).
4. S. Krishna, J. Phys. D: Appl. Phys. **38**, 2142 (2005).
5. S. Raghavan, D. Forman, P. Hill, et al., J. Appl. Phys. **96**, 1036 (2004).
6. E.-T. Kim, A. Madhukar, Z. Ye, and J. C. Campbell, Appl. Phys. Lett. **84**, 3277 (2004).
7. P. Bhattacharya, X. H. Su, S. Chakrabarti, et al., Appl. Phys. Lett. **86**, 191106 (2005).
8. L. D. Moldavskaya, V. M. Daniltsev, M. N. Drozdov, et al., in *Proceedings of 12th International Conference on Narrow Gap Semiconductors, Toulouse, France, 2005*, Ed. by J. Kono and J. Léotin (Taylor and Francis, London, 2006), p. 360, Inst. Phys. Conf. Ser., No. 187.
9. D. Fekete, H. Dery, A. Rudra, and E. Kapon, J. Appl. Phys. **99**, 034304 (2006).
10. J. F. Chen, R. S. Hsiao, Y. P. Chen, et al., Appl. Phys. Lett. **87**, 141911 (2005).
11. A. Passaseo, R. Rinaldi, M. Longo, et al., J. Appl. Phys. **89**, 4341 (2001).
12. V. M. Ustinov, Fiz. Tekh. Poluprovodn. (St. Petersburg) **38**, 963 (2004) [Semiconductors **38**, 923 (2004)].
13. A. A. El-Emawy, S. Birudavolu, P. S. Wong, et al., J. Appl. Phys. **93**, 3529 (2003).
14. S. J. Lee, S. K. Noh, K.-S. Lee, and J. W. Choe, Solid State Commun. **132**, 115 (2004).
15. D. S. Sizov, M. V. Maksimov, A. F. Tsatsul'nikov, et al., Fiz. Tekh. Poluprovodn. (St. Petersburg) **36**, 1097 (2002) [Semiconductors **36**, 1020 (2002)].
16. N. Nuntawong, S. Huang, Y. B. Jiang, et al., Appl. Phys. Lett. **87**, 113105 (2005).
17. I. N. Kaiander, R. L. Sellin, T. Kettler, et al., Appl. Phys. Lett. **84**, 2992 (2004).
18. G. Saint-Girons, G. Patriarche, L. Largeau, et al., J. Cryst. Growth **235**, 89 (2002).
19. A. Lenz, H. Eisele, R. Timm, et al., Appl. Phys. Lett. **85**, 3848 (2004).
20. V. I. Shashkin, V. M. Danil'tsev, M. N. Drozdov, et al., Fiz. Tekh. Poluprovodn. (St. Petersburg) **40**, 455 (2006) [Semiconductors **40**, 449 (2006)].
21. V. I. Shashkin, V. M. Daniltsev, Yu. N. Drozdov, et al., in *Proceedings of EW MOVPE VIII* (Prague, 1999), p. 159.
22. G. Costantini, A. Rastelli, C. Manzano, et al., Phys. Rev. Lett. **96**, 226106 (2006).
23. S. J. Lee, J. O. Kim, S. K. Noh, et al., J. Cryst. Growth **284**, 39 (2005).
24. I. A. Karpovich, N. V. Baidus, B. N. Zvonkov, et al., Nanotechnology **12**, 425 (2001).
25. H. Zhu, Z. Wang, H. Wang, et al., J. Cryst. Growth **197**, 372 (1999).
26. H. Lim, W. Zhang, S. Tsao, et al., Phys. Rev. B **72**, 085332 (2005).
27. K. Drozdowicz-Tomsiaa, E. M. Goldys, Lan Fu, and C. Jagadish, Appl. Phys. Lett. **89**, 113510 (2006).

*Translated by É. Smorgonskaya*